LA-UR-01-0442

Approved for public release; distribution is unlimited.

Title: TIME-REVERSED, FLOW-REVERSED BALLISTICS SIMULATIONS

Author(s): Louis Zernow, Zernow Technical Services, Inc.

Edward J. Chapyak and Robert P. Godwin, Applied Physics Division, LANL

Daniel R. Scheffler, Army Research Laboratory, APG

Submitted to: Proceedings of the 19th International Symposium on Ballistics, Interlaken, Switzerland, May 7-11, 2001

Los Alamos
NATIONAL LABORATORY

TIME-REVERSED, FLOW-REVERSED BALLISTICS SIMULATIONS: DO THEY HAVE POTENTIAL FOR BALLISTICS DESIGN?

L. Zernow[1], E. J. Chapyak[2], R. P. Godwin[2], and D. R. Scheffler[3]

[1] *Zernow Technical Services, Inc., San Dimas, CA, 91773, USA*
[2] *Los Alamos National Laboratory, Los Alamos, NM, 87545, USA*
[3] *Army Research Laboratory, Aberdeen Proving Ground, MD, 21005, USA*

Two-dimensional simulations of planar sheet jet formation are studied to examine the hydrodynamic issues involved when simulations are carried out in the inverse direction, that is, with reversed time and flow. Both a realistic copper equation of state and a shockless equation of state were used. These studies are an initial step in evaluating this technique as a ballistics design tool.

HISTORICAL INTRODUCTION

In 1994, Pai and Kuz'min [1] discussed the dynamic measurement of jet temperatures using a clever thermoelectric method deploying a transverse thermocouple interface in the jet generated by a bimetallic hemispherical liner. They did not describe the interfacial geometry of the bimetallic components of the liner. One of us (LZ) was interested in carrying out this experiment with a uniform wall conical liner to compare its results with previously published jet temperature measurements [2,3]. A non-iterative method for defining the required interface geometry for a conical liner, which would generate such a bimetallic interface in the jet, already existed [4]. In considering this problem, it was natural to ask, "Under what conditions might this computational problem be run backward in time, with reversed flow, in order to define the bimetallic interface in the original liner?" If the reversed-time reversed-flow (RT-RF) problem were generalized and could be successfully computed, it could lead to potentially useful design capabilities. It was clear that this approach would present difficult thermodynamic challenges. An initial discussion ensued between two of the authors (LZ and EJC) in 1995 and they found that, earlier, the third author (RPG) had discussed the contemplated method and applied it to a simplified version of a Birkhoff jet [5]. In Godwin's forward running example, a sheet jet and a sheet slug were formed by two flat plates colliding with each other at a specified acute angle 2β [6]. In 1992, Godwin had

recognized the potential value of the RT-RF method and commented, "Since there are practical problems for which we wish to produce a particular solution, running problems backward may be a useful technique." He also recognized that an inverse jet is essentially identical to a forward running kinetic energy penetrator. The Birkhoff 2-D Cartesian planar jet is the analog of a cylindrical long-rod penetrator in the limit of an infinitely thick slug sheet.

This paper will briefly discuss the "Lagrangian Tracer Particle" technique for solving the thermocouple deployment problem. It will then summarize Godwin's results for the simplest 2-D jet problem using the RT-RF technique. The jet-slug configuration obtained from the forward problem will be compared with solutions obtained from the inverse simulation with flow conditions under which the inverse simulation technique should produce results identical to those of the forward problem. The introduction of artifacts, such as extraneous shocks, in the application of the RT-RF method, when using realistic material models, will be noted. These artifacts due to irreversible effects are not generated in the forward problem. The results obtained by deliberate selection of a simplified, shockless equation of state (EOS), which minimizes this problem, will also be discussed.

The essential hydrodynamics occurs in the collision zone in the region around the collapse angle β. The engineering definition of a shaped-charge liner and its integration into the rest of a warhead is recognized as important for practical design. This portion of the design analysis involves mainly non-hydrodynamic issues and will not be addressed in this paper. However, aspects of warhead design that involve the interactions of the explosive with the complete warhead configuration must ultimately be considered. A preliminary examination of one approach to this next design phase has been carried out by the fourth author (DRS) using rigid, inelastic guiding templates to redirect and curve the outward reverse flow, along the direction of the collapse angle β, into the original liner wedge angle α, ($\alpha < \beta$). Scheffler began his study by examining the simplest sliding interface problem with CTH, an Eulerian code. He observed the expected computational problems, concluding that, for this flow-guidance requiring an excellent sliding interface, a Lagrangian code would be more suitable than an Eulerian code [8]. Since this part of the design process involves the choice of explosive, it could be handled by a computation of the forward-running plate-deflection problem, which turns α into β. However, even in plane strain, this is difficult, since the required profile for a liner of non-uniform thickness has not been defined. Deriving liner designs for axi-symmetric jets and EFP's poses interesting and taxing problems, such as liner thickness changes that occur during the radial liner collapse of cylindrical warheads. We focus on the basic hydrodynamic problems involving simple plane strain in the vicinity of the collision

zone. We will briefly discuss work directed toward solving generalized "adjoint hydrodynamics" equations for use in design [9].

USING LAGRANGIAN TRACER PARTICLES FOR LINER DESIGN

Reference [1] discusses a hemispherical liner which places a thermocouple interface in the jet, but the interface design is not specified. Reference [4] describes a technique for designing a bimetallic conical liner interface for deploying a thermocouple in a jet. It utilizes multiple (e.g., 10) rows of tracers, each row containing equidistant tracer particles with up to 99 individually identifiable Lagrangian tracer particles. These rows of tracers are computationally located in equidistant parallel rows, across the initial liner thickness, and perpendicular to the liner surfaces. By running the problem in the forward direction, with the tracers systematically placed in the original liner, and observing the final location of the tracer particles within the jet, the desired initial location of the bimetallic interface points in the liner can be identified in a single numerical simulation.

COMPARISON OF FORWARD AND TIME-REVERSED SIMULATIONS

As shown in the classic paper by Birkhoff, et al. [7,10], the flows associated with a planar jet formed by the collision of two plates in 2-D Cartesian coordinates can be modeled assuming steady-state incompressible flow when the "hinge" angle is above a critical value [11]. For an EOS of the ideal gas form, the critical angle β_c is $\tan\beta_c \le \left(\gamma^2 - 1\right)^{-1/2}$ [12,13]. Using $\gamma = \Gamma + 1 \sim 3$, where Γ is the Grüneisen gamma of metals, $\beta_c \le 19.5°$. The application of Bernoulli's law along the central streamline is the essential feature of the Birkhoff paradigm. The model qualitatively describes the conical metal liners of shaped-charge munitions. However, due to mass convergence, a cylindrical fixed-thickness liner does not allow the choice of a moving frame with a stationary hinge. Since Bernoulli's law contains only the square of velocities, the streamline equations for isentropic flow are invariant under time reversal. A reverse Birkhoff jet can be realized in the edge-on collision of thick (slug) and thin (jet) sheets. Forward and reverse time simulations of the Birkhoff model were used in validating numerical tools and investigating compressible dynamics and the associated shocks on jet formation [5,6]. We review those studies here to assess the potential of time-reversed simulations in munition design, that is, of working backward from a desired final jet configuration to the corresponding initial conditions.

The Chaplygin EOS used in our simulation studies provides a useful approximation to jet dynamics even though it cannot address shock physics [13].

Karpp used this EOS in an analytical study of compressible effects on jet dynamics [14]. The failure of this EOS to model shocks is less serious than it might appear. Table 1 gives analytical predictions for a copper Birkhoff jet with incompressible flow and with compressible Chaplygin flow using various parameter choices. Notice that, with C_o=100 km/s, the pressure, density, and internal energy approximate those of incompressible flow. Table 2 summarizes MESA2D simulation results with a realistic Cu EOS and with the Chaplygin EOS using C_o=10 and 100 km/s; both forward and time-reversed simulations are tabulated. Details of the EOS assumptions and simulations are described in the Appendix. As expected, the peak pressure, density, and internal energy density of the Chaplygin simulation with C_o=100 km/s approach those of the Birkhoff model with incompressible flow. The simulation using C_o=10 km/s is qualitatively similar to that with a realistic Cu EOS. The analytical values for C_o=7 km/s show that important parameters for realistic Cu can be matched by an appropriate C_o choice. (The small differences between the forward and reverse simulations presumably result from minor differences in numerical zoning, not allowing sufficient simulation time for transients to relax, etc. The maximum flow velocities in the simulations slightly exceeded the expected steady-state value. No attempt was made to eliminate these minor numerical artifacts.)

In Fig. 1, we have plotted material interfaces and isobars near the hinge for the forward and time-reversed simulations with a realistic Cu EOS. The forward and reversed simulations of 1a and 1b are qualitatively similar, but differ quantitatively. The slug and jet flows away from the hinge in 1a are not exactly parallel to the axis because an orthogonal velocity component has been introduced by the irreversible energy deposition due to a shock. Similarly, shock heating in the time-reversed simulation causes the outgoing flow in the "arm" of 1b to spread. The material interface in the time-reversed flow explicitly distinguishes the portion of the flow originating in the jet, a feature potentially useful in design. Pressure profiles in the hinge region (isobars $\geq$ 0.7Mbar) for the two simulations are essentially identical. On the other hand, at pressures $\leq$ 0.35Mbar, isobars for the two situations have a different character because of the pressure discontinuity across the shock in the incoming arm (slug) of the forward (reversed) simulation. Figure 2a displays the isobars for a forward Chaplygin simulation with C_o=10 km/s. (The plot for the corresponding time-reversed simulation is indistinguishable from 2a.) There are no dissipative shocks when using the Chaplygin EOS. Thus, there is no material heating, no spreading of the outgoing flows, and no convergence of isobars such as that associated with the shocks in 1a and 1b.

TABLE 1. Predictions for a Cu jet with β=20° and a plate velocity of 2 km/s (V_2 =5.495 km/s).

	Birkhoff	$C_o = V_2$	C_o =7 #	C_o =10	C_o =100
Pressure (Mbar)	P_B=1.348	$2P_B$ =2.696	1.505	1.450	1.349≈ P_B
η_{max}	0	1	0.344	0.151	1.51×10^{-3}
ρ_{max} (g/cm^3)	ρ_o=8.930	∞	13.61	10.52	8.944≈ ρ_o
i	0	0.151	0.029	1.14×10^{-2}	1.14×10^{-4}

i = internal energy density (Mbar·cm^3) # (km/s)

TABLE 2. Simulation results using a realistic Cu EOS and the Chaplygin EOS.

	Realistic U_s/u_p		Chaplygin, C_o=10		C_o=100
	forward	reverse	forward	reverse	forward
Pressure (Mbar)	1.786	1.740	1.461	1.451	1.344
ρ_{max} (g/cm^3)	13.72	13.62	10.68	10.66	8.944
i	0.0237	0.0235	0.0138	0.0152	1.13×10^{-4}

CONCLUSIONS

Aside from features associated with shock waves, simulation results obtained using a Chaplygin EOS resemble those obtained with a realistic EOS. The similarity is particularly good near the stagnation and hinge points, which we presume to be important locations in shaped-charge design. The shock pressures are small compared to the stagnation pressures, the energy dissipated by shocks is small, and the shocks are spatially separated from the stagnation points. These features help make the incompressible flow Birkhoff model such a useful jet paradigm. Our studies suggest using the following procedure may prove useful in time-reversed design. After selecting a final jet configuration as the initial problem geometry, choose a Chaplygin EOS for use in a reversed-time simulation. Then, to account for the effects of shocks, strength, etc., run a forward simulation using the best available material response models with the output geometry of the reversed-time simulation as the initial geometry. Simulations in cylindrical and spherical geometry will not be as simple as those of a Cartesian problem, which assumes steady-state flow, but we do not believe this will prevent useful design guidance from being obtained through time-reversed simulations.

We note the continuing development of a promising abstract approach, adjoint hydrodynamics, for use in optimizing designs [9]. In adjoint hydrodynamics, physics-based partial differential equations (PDEs) are differentiated with respect to the parameters of interest and transformed into adjoint PDEs. Initial applications of

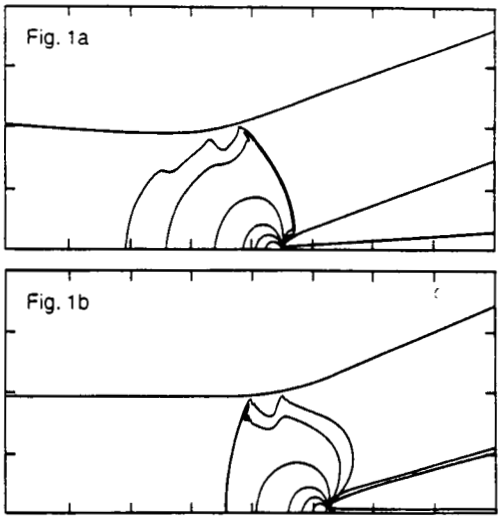

FIGURE 1. Material interfaces and isobars for the forward (a) and reversed (b) simulations with a realistic Cu EOS. Isobars at 0.175, 0.350, 0.700, 1.00 and 1.20 Mbar. Note the spreading of the jet and slug in (a) and the "arm" in (b). The grid ticks are 2 mm. The incident plate ("arm") is 4 mm thick in the forward simulations.

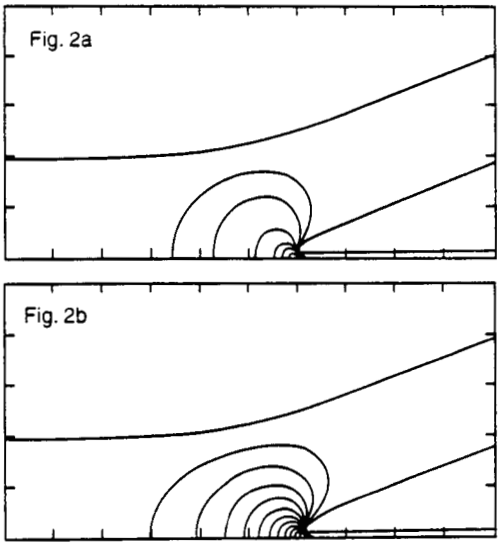

FIGURE 2. Simulations using the Chaplygin EOS with C_o=10 (a) and 100 km/s (b). Isobars in (a) are identical to those of Fig. 1; in (b) the isobars range from 0.122 to 1.22 Mbar in steps of 0.122 Mbar. Ticks are 2 mm. Note the absence of shocks; (b) closely approximates the incompressible flow Birkhoff jet paradigm.

this technique proved to be unsatisfactory, but the development of automatic differentiation tools has improved its accuracy. Birkhoff jet formation serves as a test problem for validating numerical adjoint Jacobians. Comparisons of computational resource requirements for conventional and adjoint simulations indicate that the adjoint technique will become efficient when addressing complex design issues involving many parameters. Using adjoint design can, in principle, account for shocks and other irreversible processes.

APPENDIX

Using the notation of Birkhoff, et al., we simulated the collision of two flyer plates with a half hinge angle β. In a moving frame, where the hinge point is at rest, the jet and slug recede from the stagnation point with the same speed (V_2) as the plate material approaches. In the laboratory frame, the jet and slug velocities are

$$V_j = V_o(1+\cos\beta)/\sin\beta \quad \text{and} \quad V_s = V_o(1-\cos\beta)/\sin\beta; \tag{A1}$$

V_o is the colliding plate velocity in the laboratory frame. In the frame in which the hinge point is stationary,

$$u_x = -V_2\cos\beta = -V_o\cos^2\beta/\sin\beta \quad \text{and} \quad u_y = -V_2\sin\beta = -V_o\cos\beta. \tag{A2}$$

Bernoulli's law gives the maximum stagnation pressure

$$P_B = \rho_o V_2^{\,2}/2 = \rho_o V_o^{\,2}/(2\tan^2\beta). \tag{A3}$$

To simulate a copper jet, we chose β=20°, V_o=2 km/s, and ρ_o=8.93 g/cm^3 which yield V_2=5.495 km/s (with corresponding jet and slug velocities of 12 and 0.3 km/s) and P_B=1.348 Mbar =134.8 GPa.

Neglecting material strength, a linear U_s/u_p Grüneisen EOS [15], $U_s=C_o+u_p$, provides realistic copper modeling with C_o=3.94 km/s, s=1.489, ρ_o=8.93 g/cm^3, and Grüneisen Γ=2.002. The numerical simulation of an incompressible fluid requires an infinite sound speed, which would cause our hydrodynamics code, MESA2D [16], and similar codes to assume computational time steps of zero and stop. To approach incompressible fluid behavior for comparison of simulations with the Birkhoff model, we chose a simplified linear U_s/u_p EOS with s=0 and an unrealistically large C_o. This EOS is of the Chaplygin form with unique features; it supports neither compressive shock waves nor supersonic flow and its density is a function of velocity only [13]. We used this EOS to provide an asymptotic approach to inviscid incompressible behavior. With our EOS assumptions,

$$P = \rho_o C_o^2\eta \quad \text{and} \quad c^2 = \partial P/\partial\rho = \rho_o^2 C_o^2/\rho^2 = C_o^2(1-\eta)^2, \tag{A4}$$

where $\eta \equiv 1-\rho_o/\rho$. (The pressure behind a shock and shock velocity with the conventional U_s/u_p EOS are $P=\rho_o C_o^2\eta(1-s\eta)^{-1}$ and $U_s = C_o\left[1+s\eta(1-s\eta)^{-1}\right]$, respectively.) In 2-D steady-state flow, we have along a streamline [17]

$$udu + vdv = -c^2 d\rho/\rho. \tag{A5}$$

Assuming the y component of velocity, v, and its derivative are zero along the x axis and and noting that $c^2 d\rho = dP$ gives Bernoulli's law the form

$$\int_u^{V_2} udu = -\int_P^0 dP/\rho \quad \text{or} \quad \int dP/\rho = \left(V_2^2 - u^2\right)/2. \tag{A6}$$

Using the pressure of Eq. (A4)

$$\int dP/\rho = \left(\rho_o C_o\right)^2 \int_\rho^{\rho_o} \rho^{-3} d\rho = \frac{C_o^2}{2}\left(1 - \rho_o^2/\rho^2\right) \tag{A7}$$

yielding the quadratic

$$P^2 - 2\rho_o C_o^2 P + (\rho_o C_o)^2 (V_2^2 - u^2) = 0 \qquad \text{(A8)}$$

with the solution

$$P = \rho_o C_o^2 \left[1 \pm \sqrt{1 - (V_2^2 - u^2)/C_o^2} \right]. \qquad \text{(A9)}$$

When $V_2 << C_o$, the maximum pressure (at u=0) approaches P_B, the Bernoulli stagnation pressure, and η approaches zero corresponding to incompressible dynamics. When $V_2 = C_o - \Delta V$, with $\Delta V << V_2, C_o$, the stagnation pressure approaches $2P_B$ and $\eta \rightarrow 1$, representing compression to infinite density. In metal jet formation, $V_2 \geq 2C_o$, a situation which cannot be reproduced with the Chaplygin EOS, since it precludes supersonic flow. The compressibilities reached can, however, be matched using the Chaplygin EOS. From thermodynamics, the specific internal energy

$$di = -PdV + \Delta Q = pd\rho/\rho^2 \quad \text{or} \quad i = C_o^2 \int_0^\eta \eta d\eta + Q = C_o^2 \eta^2/2 + Q. \qquad \text{(A10)}$$

For insentropic flow (Q=0), the internal energies of the nearly incompressible and very compressible cases approach 0 and $V_2^2/2$, respectively, near the stagnation point.

REFERENCES

1 V. V. Pai and G. E. Kuz'man, *Combustion, Explosives and Shock Waves*, **30**(3), 346-349, 1994.

2 W. G. von Holle and J. J. Trimble, "Shaped-Charge Temperature Measurement," *Proc. 6th Int. Symposium on Detonation*, **1**, 691-699, 1976.

3 L. Zernow and R. H. Zernow, "Experimental...Temperature of Shaped-Charge Jet...," *15th Int. Symposium on Ballistics*, Jerusalem, Israel, May 1995.

4 L. Zernow, E. J. Chapyak, K. Meyer and R. H. Zernow, "The Origins of Liner Material in a Shaped-Charge Jet Particle," *13th Int. Symposium on Ballistics*, Stockholm, Sweden, June 1992.

5 R. P. Godwin, "Inverse Simulations of Birkhoff Jets," Los Alamos National Laboratory Internal Memorandum, X-3:92-283U, November 1992.

6 R. P. Godwin, "Simulations of Birkhoff Jets," Los Alamos National Laboratory Internal Memorandum, X-3:92-282U, November 1992.

7 G. Birkhoff, D. P. MacDougall, E. M. Pugh, and G. I. Taylor, *J. Appl. Phys.* **19**, 563-582, 1948.

8 D. R. Scheffler and J. A. Zukas, "Practical Aspects of Numerical Simulations of Dynamic Events: Material Interfaces," Army Research Laboratory Report, ARL-TR-2302, September 2000.

9 R. Henninger, M. L. Rightley and P. J. Maudlin, *Shock Compression of Condensed Matter – 1999* (AIP Conf. Proc.), ed. by M. D. Furnish, L. C. Chhabildis and R. S. Hixson, 359-362, 2000.

10 W. P. Walters and J. A. Zukas, **Fundamentals of Shaped Charges** (J. Wiley & Sons, 1989).

11 J. M. Walsh, R. G. Shreffler and F. J. Willig, *J. Appl. Phys.* **24**(3), 349-359, 1953.

12 F. H. Harlow and W. E. Pracht, *Phys. Fluids,* **9**(10), 1951-1959, 1966.

13 L. D. Landau and E. M. Lifshitz, **Fluid Mechanics**, 1st ed. (Pergamon, 1959)

14 R. R. Karpp, *Quarterly of Appl. Math.*, **42**(1), 15-20, 1984.

15 W. B. Harvey, "Attenuation of Shock Waves in Copper and Stainless Steel," Los Alamos National Laboratory Report, LA-10753-T (thesis, 1980).

16 K. S. Holian, D. A. Mandell, T. F. Adams, F. L. Adessio, J. R. Baumgardner and S. J. Mosso,"MESA: Computer Code for Armor/Anti-Armor Applications," *Proc. Supercomputing World Conference*, San Francisco, CA, October 1989.

17 R. Courant and K. O. Friedricks, **Supersonic Flow and Shock Waves** (Interscience, 1940).